Eur. J. Mineral.
2003, **15**, 469–473

Thermal expansion of natural orthoenstatite to 1473 K

JENNIFER M. JACKSON[1]*, JAMES W. PALKO[2], DENIS ANDRAULT[3], STANISLAV V. SINOGEIKIN[1], DMITRY L. LAKSHTANOV[1], JINGYUN WANG[1], JAY D. BASS[1], and CHANG-SHENG ZHA[4]

[1]Department of Geology, University of Illinois, Urbana, IL 61801, U.S.A.
*Corresponding author, e-mail: jmjackso@uiuc.edu
[2]Department of Materials Science and Engineering, University of Illinois, Urbana, IL 61801, U.S.A.
[3]Laboratoire des Géomatériaux, Institut de Physique du Globe de Paris, 4 place Jussieu, F-75252 Paris Cedex 05, France
[4]Cornell High Energy Synchrotron Source (CHESS), Cornell University, Ithaca, NY 14853, U.S.A.

Abstract: The volume thermal expansion of powdered natural orthoenstatite [$(Mg_{0.994}Fe_{0.002}Al_{0.004})_2(Si_{0.996}Al_{0.004})_2O_6$] has been measured to 1473 K using energy dispersive synchrotron X-ray diffraction. Over the temperature range examined, the data are consistent with a volume thermal expansion, α, that linearly increases with temperature as given by the expression $\alpha(T) = 29.7(16) \times 10^{-6} K^{-1} + 5.7(11) \times 10^{-9} K^{-2} T$. An analysis in terms of the often-used constant expansion coefficient yields $\alpha_0 = 34.5(17) \times 10^{-6} K^{-1}$, which is in good agreement with several previous experimental results on orthoenstatite ($Mg_2Si_2O_6$) over a similar temperature range. Our results do not support the extreme upper and lower bounds reported in earlier studies for the thermal expansivity of Fe-rich orthoenstatite, but rather suggest that the thermal expansion of this phase is approximately midway between those extreme values.

Key-words: orthoenstatite, thermal expansion, high-temperature, X-ray diffraction.

1. Introduction

Orthopyroxene, with a simplified formula of $(Mg,Fe)_2Si_2O_6$, is abundant in mafic rocks of Earth's crust and upper mantle. Therefore, the behavior of this material at high temperature is important for constraining the properties of such rocks at high temperature, as well as the density of possible upper mantle mineral assemblages. The thermal expansion is also required to calculate elastic moduli from high-temperature velocity measurements, such as those obtained by Brillouin scattering or ultrasonic interferometry. The accuracy of high-temperature elasticity results is directly linked to the accuracy with which the thermal expansion is known (*e.g.*, Jackson *et al.*, 2000; Li *et al.*, 1998; Isaak *et al.*, 1992).

Numerous previous studies, using a variety of experimental techniques and sample compositions, have been carried out to determine the thermal expansion of orthoenstatite. The results of those studies are most often presented in terms of a constant volume thermal expansion coefficient (α_0), with reported results ranging from 20.8(16) to 47.7 × $10^{-6} K^{-1}$ (Table 1). It is not known whether the broad range of reported expansivities is due to the different types of samples used (*e.g.*, polycrystalline *versus* single crystals), differences in the measurement methods, differences in the chemical compositions of the samples, or combinations of all these factors.

Given the high level of uncertainty implied by the previous results, we undertook an experimental study of the volume thermal expansion of $Mg_2Si_2O_6$ orthoenstatite with near end-member composition, by powder X-ray diffraction using synchrotron radiation.

2. Experimental

2.1 Sample description

The orthoenstatite crystals used in this study are from Zabargad Island, Egypt (Kurat *et al.*, 1993). The specimens consisted of colorless, euhedral, gem-quality orthoenstatite crystals. Electron microprobe analyses (EMPA) were performed to determine the composition, using a Cameca SX-50 instrument in wavelength-dispersive mode. All EMPA runs were performed with an accelerating voltage of 15 kV and a probe current of 25 nA. Counting times on peak and background were 10 to 20 s for the following elements: Ti, Cr, Mg, Al, Si, Ca, Fe, and Mn *K*α. Identical analytical conditions were used to analyze both the standards and the orthoenstatite crystals. All iron is assumed to be FeO. The average of nine EMPA analyses for three crystals gives the following results in weight percents (standard deviations obtained from analyses on three orthoenstatite crystals are reported in parentheses): SiO_2, 58.7(5); MgO, 40.2(4); Al_2O_3, 0.4(1); FeO, 0.16(4); Cr_2O_3, 0.03(1); CaO, 0.010(7); MnO, 0.01(1); and TiO_2, 0.004(5). A 100 s energy-dispersive scan indicated that no elements with Z greater than eight, other

DOI: 10.1127/0935-1221/2003/0015-0469
0935-1221/03/0015-0469 $ 2.25

Table 1. Experimentally determined volume thermal expansion coefficients (α_0) for orthoenstatite.

Ref.	Sample description	Method	Range T (K)	α_0 (x10^{-6} K^{-1})
1	Natural pwd: $(Mg_{.994}Fe_{.002}Al_{.004})_2(Si_{.996}Al_{.004})_2O_6$	EDX	300 – 1473	34.5(17)*
2	Synthetic pwd: $Mg_2Si_2O_6$	ADX	293 – 1094	32.2(11)
3	Synthetic sc: $Mg_2Si_2O_6$ (0.42 wt% $Li_2O+V_2O_5$)	ADX	298 – 1000	30.7†
4	Synthetic sc: $Mg_2Si_2O_6$ (0.42 wt% $Li_2O+V_2O_5$)	ADX	296 – 1300	23.5 – 48.8S
4	Synthetic sc: $(Mg_{.8}Fe_{.2})_2Si_2O_6$	ADX	296 – 1300	24.2 – 48.2S
5	Natural poly: $(Mg_{.852}Fe_{.133}Ca_{.012}Mn_{.003})_2Si_2O_6$	Dilat	173 – 1073	20.8(16)
6	Natural pwd: $(Mg_{.8}Fe_{.2})_2Si_2O_6$	ADX	298 – 1273	47.7
7	Synthetic poly: $Mg_2Si_2O_6$ (2 wt% LiF)	Dilat	573 – 973	36

Notes: [1] This study, [2] Hugh-Jones (1997), [3] Zhao *et al.* (1995), [4] Yang & Ghose (1994), [5] Dietrich & Arndt (1982), [6] Frisillo & Buljan (1972), [7] Sarver & Hummel (1962).

EDX: energy-dispersive X-ray diffraction, ADX: angle-dispersive X-ray diffraction, Dilat: dilatometry, pwd: powder, sc: single crystal, poly: polycrystalline.

* We obtain $\alpha(T) = 29.7(16) \times 10^{-6} K^{-1} + 5.7(11) \times 10^{-9} K^{-2} T$ from a quadratic fit to our high temperature volume data (see text for discussion).

† thermal expansion evaluated at 298 K using: $\alpha(T) = 28.6(29) \times 10^{-6} K^{-1} + 7.2(16) \times 10^{-9} K^{-2} T$

S The range of values reported for a temperature dependent expansivity.

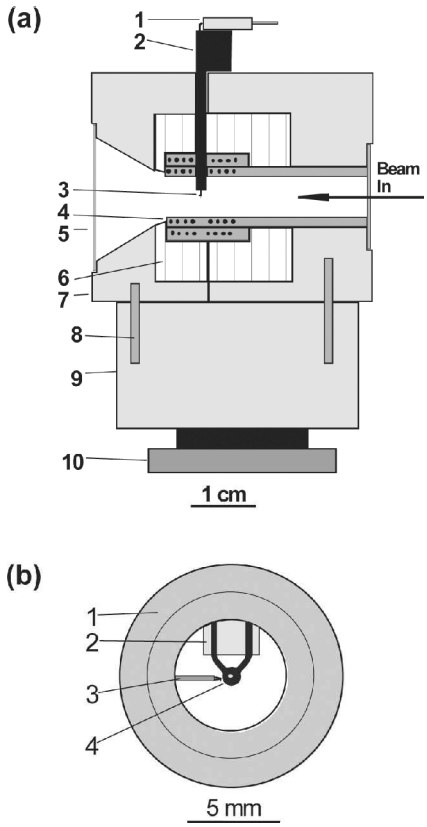

Fig. 1. (a) High-temperature ceramic furnace for synchrotron X-ray measurements. 1: thermocouple connector, 2: ceramic thermocouple/sample holder, 3: thermocouple junction with embedded sample (see Fig. 1b), 4: heating elements, 5: silica glass window, 6: insulating ceramic fiber tape, 7: ceramic furnace body, 8: pins, 9: ceramic base, 10: metal base for mounting the furnace. (b) Detector-side schematic view of the heater and sample assembly. 1: high-alumina ceramic heater, 2: removable thermocouple/sample holder, 3: control K-type thermocouple, 4: R-type thermocouple junction with the powder sample in a central hole.

than those reported here, are present in the orthoenstatite. The chemical formula was calculated assuming an ideal cation:anion ratio of 4:6, that all of the iron resides on octahedral sites, and the Al is divided equally onto octahedral and tetrahedral sites. The resulting simplified chemical formula is $(Mg_{0.994}Fe_{0.002}Al_{0.004})_2(Si_{0.996}Al_{0.004})_2O_6$. Polarized IR spectral analyses performed on orthoenstatite from the same locality indicates a hydrous content of 70 wt. ppm OH^- (Skogby *et al.*, 1990).

2.2 High-temperature furnace

We designed and built a compact ceramic high-temperature furnace for our high-temperature powder X-ray diffraction measurements (Fig. 1). The main body of the furnace is constructed from machinable alumina-silicate ceramics and is a modification of the furnace described by Sinogeikin *et al.* (2000) for Brillouin scattering measurements. The furnace used in the present work allows the collection of energy- and angle-dispersive ($2\theta \leq 40°$) X-ray spectra on powder samples to temperatures in excess of 1700 K. Compared with the heater for Brillouin scattering, the present design allows higher temperatures to be attained with lower thermal gradients due to a larger length-to-diameter ratio of the heater body (~1.5). The heating element consists of a platinum-rhodium ($Pt_{70}Rh_{30}$) wire (0.01" diameter), which is wound into the threads on two concentric high-alumina ceramic tubes. The side openings of the cell are covered with ~100 μm thick fused silica windows to increase thermal efficiency and to minimize thermal gradients. The experiments in this study were performed in air, although it is possible to control the atmosphere in this furnace.

For the high-temperature X-ray diffraction measurements, several orthoenstatite crystals with no visible inclusions were ground to a powder under ethanol using an agate mortar and pestle. Although grinding can sometimes induce partial transformation of orthoenstatite (space group *Pbca*, *e.g.* Yang & Ghose, 1995) to low clinoenstatite ($P2_1/c$, *e.g.* Stephenson *et al.,* 1966) (Lee & Heuer, 1987), a room-temperature Rietveld refinement of high-resolution angle-dispersive X-ray diffraction data on the powder used for our experiments indicated that only orthoenstatite was present. The powder was packed into a hole (350 μm in diameter) drilled in a flattened and annealed R-type thermocouple junction that was used for our temperature measurements

(Fig. 1b). This setup helps ensure that the uncertainty in sample temperature is within the accuracy of the thermocouple reading. The thermocouple with the sample was attached to an alumina ceramic holder, which was centered in the heater. An additional thermocouple (K-type) was placed near the sample and provided redundant temperature measurements. The maximum difference between the two thermocouple measurements was about 4 K.

2.3 In-situ high-temperature synchrotron X-ray diffraction

Energy-dispersive X-ray diffraction (EDX) measurements at high temperatures were performed on the bending magnet beamline station B1 at the Cornell High Energy Synchrotron Source (CHESS). The incident X-ray beam was reduced to 40 μm via horizontal and vertical slits. The downstream collimator for the diffracted X-rays consisted of two vertical slits. The front slit is 70 μm wide, 0.5 mm high, and 37 mm away from the sample; the back slit is 300 μm wide, 1 mm high, and positioned in the front of the detector. The two slits are separated by more than 0.5 m. All EDX measurements were made using a fixed 2θ angle of 12.006° and a high-resolution intrinsic Ge detector. The value of the 2θ diffraction angle was calibrated using the eight strongest reflections of gold at ambient conditions. The overall beam divergence was approximately 0.65 mrad. EDX diffraction spectra on orthoenstatite were collected at room temperature (300 K), then at temperature intervals of 100 degrees upon increasing temperature from 373 to 1473 K. The temperature was then decreased to 1423 K, and EDX spectra were collected in roughly 200-degree increments from 1423 K down to room temperature.

2.4 Refinement of diffraction peaks and cell dimensions

A multi-step profile analysis was carried out using a modified version of the General Structure Analysis System (GSAS) (Larson & Von Dreele, 1988) for energy-dispersive spectra. The orthoenstatite structure (*Pbca, e.g.* Yang & Ghose, 1995) was used as a starting model for all refinements in the Rietveld mode. Final values of the lattice parameters were obtained by a Le Bail refinement (Le Bail *et al.*, 1988). During the fitting procedure, the background was refined simultaneously with peak positions to ensure that low intensity reflections were included. The final cell parameters were then used to calculate the volume for orthoenstatite at each temperature (Table 2; Fig. 2). Le Bail refinements were performed because the relative intensities of the diffraction peaks were unreliable, in part due to the relatively large grain size of the powder. This was evident from significant changes in peak intensities during re-centering of the sample, which was done after each temperature increase. The differences in lattice parameters between the Rietveld and Le Bail refinement modes were generally less than 0.1%, with the Le Bail refinement giving a significant (~10%) improvement in the reduced χ^2 (a measure of the goodness of fit) of the peak position residuals. Because the volume change due to thermal expansion is small, the slight improvement in lattice parameters from the Le Bail refinement results in a significantly higher degree of internal consistency in the high-temperature volume data. The χ^2 ranged from about 5 at low temperatures to about 12 at high temperatures, when the spectra were indexed as orthoenstatite. We also tried indexing the spectra as low clinoenstatite, as protoenstatite (*Pbcn*, *e.g.* Yang & Ghose, 1995), and as combinations of these phases. However, these refinements resulted in much higher χ^2 values ranging from 20 to 35. Therefore, we did not resolve a clear indication of a phase transition in orthoenstatite within the temperature range of this study. This may be in part due to the kinetics of the transformation (*e.g.* Yang & Ghose, 1995) or poor detector resolution.

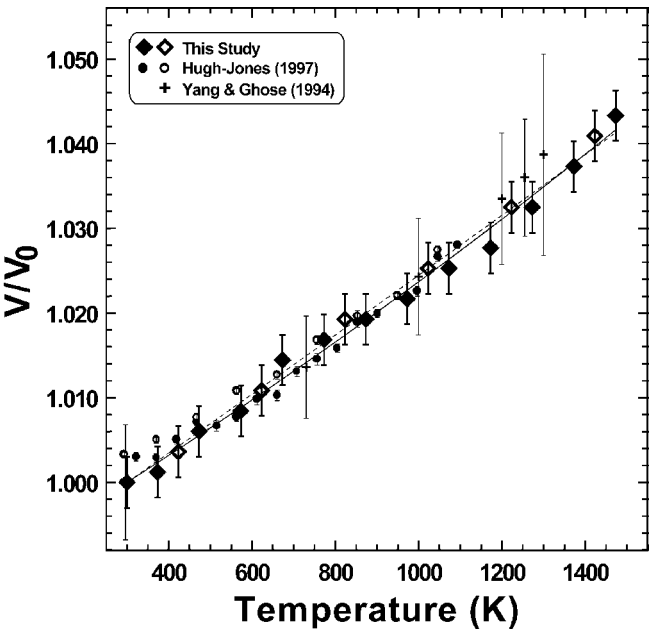

Fig. 2. Normalized unit cell volumes of orthoenstatite as a function of temperature. Open symbols were obtained on decreasing temperature. The data of Yang & Ghose (1994) are for $Mg_2Si_2O_6$. The dashed and solid lines represent fits to our data obtained from Eq. 2 (constant α), and from a quadratic fit, respectively.

3. Results and discussion

The volumetric coefficient of thermal expansion at constant pressure, α, is defined by the expression:

$$\alpha = 1/V\,(\partial V/\partial T)_P \quad \text{or} \quad V(T) = V_0 \exp[\int \alpha(T) dT], \qquad (1)$$

where V_0 is the measured volume at room temperature and $\alpha(T)$ is a temperature-dependent thermal expansion. The results of thermal expansion measurements are most often given in terms of a constant, or $\alpha(T) = \alpha_0$ (this is, in particular, true for a majority of the results on orthoenstatite referenced in this paper). In this case it follows from Eq. 1 that:

$$\ln(V/V_0) = \alpha_0 (T - T_0), \qquad (2)$$

where V_0 is the measured volume at room temperature (T_0),

Table 2. Lattice parameters and volume of orthoenstatite as a function of temperature.

T (K)	a (Å)	b (Å)	c (Å)	V (Å^3)
300	18.210(55)	8.794(55)	5.190(55)	831.1(17)
373	18.246(55)	8.810(55)	5.178(55)	832.4(17)
473	18.222(55)	8.815(55)	5.203(55)	835.7(17)
573	18.253(55)	8.830(55)	5.199(55)	837.9(17)
673	18.300(55)	8.849(55)	5.208(55)	843.3(17)
773	18.320(55)	8.860(55)	5.207(55)	845.2(17)
873	18.321(55)	8.879(55)	5.206(55)	846.9(17)
973	18.355(55)	8.875(55)	5.215(55)	849.4(17)
1073	18.384(55)	8.886(55)	5.216(55)	852.1(17)
1173	18.360(55)	8.891(55)	5.232(55)	854.2(17)
1273	18.386(55)	8.916(55)	5.236(55)	858.4(17)
1373	18.405(55)	8.924(55)	5.248(55)	862.0(17)
1473	18.510(55)	8.900(55)	5.260(55)	866.5(17)
1423*	18.455(55)	8.906(55)	5.266(55)	865.4(17)
1223*	18.394(55)	8.890(55)	5.246(55)	857.8(17)
1023*	18.392(55)	8.890(55)	5.208(55)	851.5(17)
823*	18.383(55)	8.864(55)	5.197(55)	846.9(17)
623*	18.303(55)	8.838(55)	5.193(55)	840.0(17)
423*	18.225(55)	8.803(55)	5.197(55)	833.8(17)
300*	18.196(55)	8.804(55)	5.190(55)	831.4(17)

Notes: Errors in volume are calculated based on the resolution of the solid-state Ge detector and the measured uncertainty in the 2θ diffraction angle. These uncertainties are generally larger than uncertainties in lattice parameters determined using the GSAS program. We report an insignificant number to avoid round-off error.
* decreasing temperature

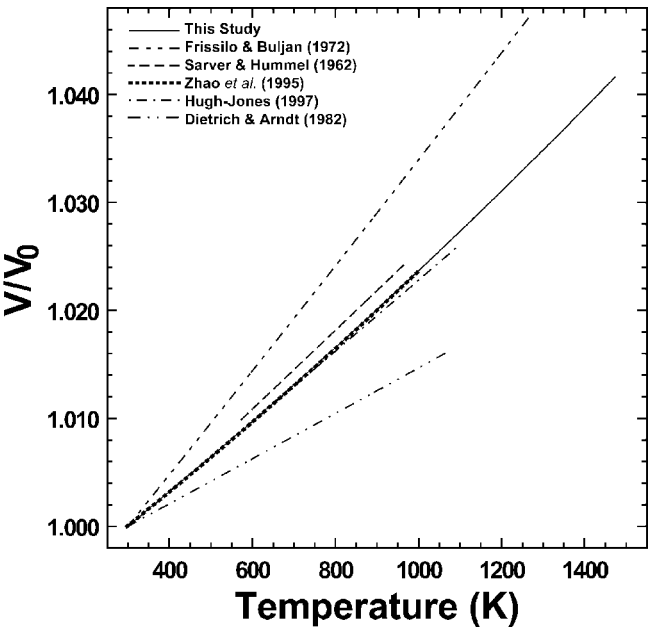

Fig. 3. Normalized volume thermal expansion curves of orthoenstatite from previous measurements. The curves for this study and Zhao *et al.* (1995) are calculated using a linear temperature dependence for α(T) (Table 1).

and V is the volume measured at high temperature (T) (Table 2). Analyzing our data using equation 2, we obtain $\alpha_0 = 34.5(17) \times 10^{-6}\,K^{-1}$ for orthoenstatite from T = 300 to 1473 K (Table 1). Note however, at temperatures above the Debye temperature [710 K for $(Mg_{0.8}Fe_{0.2})_2Si_2O_6$ (Krupka *et al.*, 1985)], the thermal expansion normally increases with increasing temperature in a nearly linear fashion (*e.g.*, Suzuki, 1975). In order to evaluate the temperature dependence of α we performed a least-squares fit of our high-temperature volume data to a quadratic function (Fig. 2). This yields a linearly increasing thermal expansion of $\alpha(T) = 29.7(16) \times 10^{-6}\,K^{-1} + 5.7(11) \times 10^{-9}\,K^{-2}\,T$ (Table 1; Fig. 3). The two models of thermal expansion yield similar calculated volumes over the temperature range of our experiments and are difficult to distinguish within the uncertainty of the data (Fig. 2). We also used the formalism described in Suzuki (1975) to fit our high-temperature volume data and obtained a temperature dependent thermal expansion that is consistent with our results for a linearly increasing α with temperature.

Within the uncertainties of the data, our results are in agreement with those of several previous studies (Sarver & Hummel, 1962; Zhao *et al.*, 1995; Hugh-Jones, 1997) (Table 1; Fig. 2 and 3). For temperatures less than about 1000 K, our results also agree with those of Yang & Ghose (1994) (Fig. 2). However, there is a significant difference between the thermal expansivity from the present study and the results of Frisillo & Buljan (1972) and Dietrich & Arndt (1982), both of whom used a Fe-rich orthopyroxene in their experiments (Table 1). Because nearly pure Mg end-member enstatite was used in the present study, the differences in thermal expansivity might be ascribed to a compositional effect of Mg-Fe substitution. However, the thermal expansion reported by Frisillo & Buljan (1972) is higher than ours by about 12×10^{-6}, and that of Dietrich & Arndt (1982) is lower than the present result by roughly an equivalent amount. Therefore, differences in composition do not appear to explain the extreme thermal expansion values of orthoenstatite reported by Frisillo & Buljan (1972) and Dietrich & Arndt (1982), and the reasons for discrepancies between these two studies are not clear. Moreover, the results of Yang & Ghose (1994) indicate that small amounts of iron should have a minimal affect on the thermal expansion of orthoenstatite (Table 1). The results of the current study confirm that the thermal expansivity of $Mg_2Si_2O_6$ orthoenstatite is approximately midway between the extreme values referred to above.

Acknowledgements: The authors would like to thank George Rossman (California Institute of Technology) for providing the orthoenstatite samples (GRR 649, AMNH 100634) and Ian Steele (University of Chicago) for providing assistance with the microprobe analysis. We thank Ross Angel, Alison Pawley, and an anonymous reviewer for comments on the manuscript, and Ross Angel, Raymond Jeanloz, Robert Finch, Donald Lindsley, George Harlow, and Jason Nicholas for helpful discussions.

References

Dietrich, P. & Arndt, J. (1982): Effects of pressure and temperature on the physical behavior of mantle-relevant olivine, orthopyrox-

ene and garnet: I. Compressibility, thermal properties and macroscopic grüneisen parameters. *in* "High-pressure researches in geoscience", W. Schreyer, ed. Schweizerbart'sche Verlagsbuchhandlung, Stuttgart, 293-306.

Frisillo, A.L. & Buljan, S.T. (1972): Linear thermal expansion coefficients of orthopyroxene to 1000°C. *J. Geophys. Res.*, **77**, 7115-7117.

Hugh-Jones, D. (1997): Thermal expansion of $MgSiO_3$ and $FeSiO_3$ ortho- and clinopyroxenes. *Am. Mineral.*, **79**, 405-410.

Isaak, D., Anderson, O.L., Oda, H. (1992): High-temperature thermal expansion and elasticity of calcium-rich garnets. *Phys. Chem. Minerals*, **19**, 106-120.

Jackson, J.M., Sinogeikin, S.V., Bass, J.D. (2000): Sound velocities of γ-Mg_2SiO_4 to 873 K by Brillouin spectroscopy. *Am. Mineral.*, **85**, 296-303.

Krupka, K.M., Robie, R.A., Hemingway, B.S., Kerrick, D.M., Ito, J. (1985): Low-temperature heat capacities and derived thermodynamic properties of anthophyllite, diopside, enstatite, bronzite, and wollastonite. *Am. Mineral.*, **70**, 249-260.

Kurat, G., Palme, H., Embey-Isztin, A., Touret, J., Ntaflos, T., Spettel, B., Brandstatter, F., Palme, C., Dreibus, G., Prinz, M. (1993): Petrology and geochemistry of peridotites and associated vein rocks of Zabargad Island, Red Sea, Egypt. *Contrib. Mineral. Petrol.*, **48**, 309-341.

Larson, A.C. & Von Dreele, R.B. (1988): GSAS manual. Los Alamos National Laboratory, report LAUR: 86-748.

Le Bail, A., Duroy, H., Fourquet, J.L. (1988): Ab-initio structure determination of $LiSbWO_6$ by X-ray powder diffraction. *Mater. Res. Bull.*, **23**, 447-452.

Lee, W.E. & Heuer, A.H. (1987): On the polymorphism of enstatite. *J. Am. Ceram. Soc.*, **70**, 349-360.

Li, B., Liebermann, R.C., Weidner, D.J. (1998): Elastic moduli of wadsleyite (β-Mg_2SiO_4) to 7 gigapascals and 873 kelvin. *Science*, **281**, 675-766.

Sarver, J.F. & Hummel, F.A. (1962): Stability relations of magnesium metasilicate polymorphs. *J. Am. Ceram. Soc.*, **45**, 152-156.

Sinogeikin, S.V., Jackson, J.M., O'Neill, B., Palko, J., Bass, J.D. (2000): Compact high-temperature cell for Brillouin scattering measurements. *Rev. Sci. Instrum.*, **71**, 201-206.

Skogby, H., Bell, D.R., Rossman, G.R. (1990): Hydroxide in pyroxene: Variations in the natural environment. *Am. Mineral.*, **75**, 764-774.

Stephenson, D.A., Sclar, C.B, Smith, J.V. (1966): Unit cell volumes of synthetic and low clinoenstatite. *Mineral. Mag.*, **35**, 838-846.

Suzuki, I. (1975): Thermal expansion of periclase and olivine, and their anharmonic properties. *J. Phys. Earth*, **23**, 145-159.

Yang, H. & Ghose, S. (1994): Thermal expansion, Debye temperature and grüneisen parameters of synthetic (Fe,Mg)SiO_3 orthopyroxenes. *Phys. Chem. Minerals*, **20**, 575-586.

– , – (1995): High temperature single crystal X-ray diffraction studies of the ortho-proto phase transition in enstatite, $Mg_2Si_2O_6$ at 1360 K. *Phys. Chem. Minerals*, **22**, 300-310.

Zhao, Y., Schiferl, D., Shankland, T.J. (1995): A high P-T single-crystal X-ray diffraction study of thermoelasticity of $MgSiO_3$ orthoenstatite. *Phys. Chem. Minerals*, **22**, 393-398.

Received 27 June 2002
Modified version received 18 November 2002
Accepted 22 January 2003